CrossMark

ORIGINAL ARTICLE

Early dynamic imaging in ^{68}Ga- PSMA-11 PET/CT allows discrimination of urinary bladder activity and prostate cancer lesions

Christian Uprimny[1] · Alexander Stephan Kroiss[1] · Clemens Decristoforo[1] · Josef Fritz[2] ·
Boris Warwitz[1] · Lorenza Scarpa[1] · Llanos Geraldo Roig[1] · Dorota Kendler[1] ·
Elisabeth von Guggenberg[1] · Jasmin Bektic[3] · Wolfgang Horninger[3] ·
Irene Johanna Virgolini[1]

Abstract

Purpose PET/CT with ^{68}Ga-labelled prostate-specific membrane antigen (PSMA)-ligands has been proven to establish a promising imaging modality in the work-up of prostate cancer (PC) patients with biochemical relapse. Despite a high overall detection rate, the visualisation of local recurrence may be hampered by high physiologic tracer accumulation in the urinary bladder on whole body imaging, usually starting 60 min after injection. This study sought to verify whether early dynamic ^{68}Ga-PSMA-11 (HBED-CC)PET/CT can differentiate pathologic PC-related tracer uptake from physiologic tracer accumulation in the urinary bladder.

Methods Eighty consecutive PC patients referred to ^{68}Ga - PSMA-11 PET/CT were included in this retrospective analysis (biochemical relapse: $n = 64$; primary staging: $n = 8$; evaluation of therapy response/restaging: $n = 8$). In addition to whole-body PET/CT acquisition 60 min post injection early dynamic imaging of the pelvis in the first 8 min after tracer injection was performed. SUV_{max} of pathologic lesions was calculated and time–activity curves were generated and compared to those of urinary bladder and areas of physiologic tracer uptake.

Results A total of 55 lesions consistent with malignancy on 60 min whole body imaging exhibited also pathologic ^{68}Ga-PSMA-11 uptake during early dynamic imaging (prostatic bed/prostate gland: $n = 27$; lymph nodes: $n = 12$; bone: $n = 16$). All pathologic lesions showed tracer uptake within the first 3 min, whereas urinary bladder activity was absent within the first 3 min of dynamic imaging in all patients. Suv_{max} was significantly higher in PC lesions in the first 6 min compared to urinary bladder accumulation ($p < 0.001$). In the subgroup of PC patients with biochemical relapse the detection rate of local recurrence could be increased from 20.3 to 29.7%.

Conclusions Early dynamic imaging in ^{68}Ga-PSMA-11 PET/CT reliably enables the differentiation of pathologic tracer uptake in PC lesions from physiologic bladder accumulation. Performance of early dynamic imaging in addition to whole body imaging 60 min after tracer injection might improve the detection rate of local recurrence in PC patients with biochemical relapse referred for ^{68}Ga-PSMA-11 PET/CT.

✉ Christian Uprimny
christian.uprimny@tirol-kliniken.at

[1] Department of Nuclear Medicine, Medical University Innsbruck, Anichstrasse 32, 6020 Innsbruck, Austria

[2] Department for Medical Statistics, Informatics and Health Economics, Medical University Innsbruck, Innsbruck, Austria

[3] Department of Urology, Medical University Innsbruck, Innsbruck, Austria

Introduction

Radical prostatectomy (RP) is an established treatment for patients with clinically localised prostate cancer (PC) [1]. In 30 to 50% of patients after RP biochemical recurrence (BR) occurs [2] defined as serum prostate-specific antigen (PSA) levels >0.2 ng/mL confirmed by two consecutive measurements [3]. However, PSA does not reliably assess the exact

site of recurrence [4, 5]. It is crucial for imaging modalities to detect local recurrence (LR) at an early stage when disease is still confined to the prostatic fossa because of higher efficacy of salvage radiotherapy [3]. Magnetic resonance imaging (MRI) has proven to be a sensitive method in detecting LR [6, 7]. On the other hand, as evaluation of the prostatic fossa with MRI using endorectal coils is limited to the pelvis, additional imaging modalities are necessary to assess the presence of LN involvement and distant metastases. Whole body PET-imaging using either C-11 or F-18 labelled choline has the potential to detect both LR and metastases [8, 9]. Unfortunately, choline PET lacks sufficient overall accuracy and sensitivity in detecting recurrent PC lesions [8, 10–15]. As the majority of PC cells show an overexpression of prostate-specific membrane antigen (PSMA) on the cell surface [16], new PET tracers targeting PSMA were designed in the past few years [17–19]. The Ga-68-labelled PSMA-ligand based on a HBED-CC conjugate of the PSMA-specific pharmacophore Glu-NH-CO-NH-Lys (^{68}Ga-PSMA-11) has especially demonstrated to be a promising PET-radiotracer in the diagnostic work-up of PC patients with BR [20–22]. With respect to the overall detection rate, ^{68}Ga-PSMA-11 PET seems to perform better than ^{18}F-choline PET [23–25].

In ^{68}Ga-PSMA-11 PET/CT a whole-body scan conducted 60 min post-injection (p.i.) is usually performed in the clinical routine [20–22, 26]. However, due to high physiologic urinary bladder activity at this time point, the detection of LR could be underestimated by ^{68}Ga-PSMA-11 PET/CT [27, 28]. In ^{18}F-choline PET dynamic acquisition within the first 8 min p.i. has the power to distinguish tumour from bladder activity, with tumour related tracer uptake occurring earlier than tracer accumulation in the urinary bladder. Early dynamic acquisition enhances the detection rate of LR in BR significantly compared to late imaging alone [9]. As both ^{68}Ga-PSMA-11 and ^{11}F-choline show predominant renal excretion tracer activity in the urinary bladder might have a negative influence on the evaluation of LR in ^{68}Ga-PSMA-11 PET too [26, 28]. In ^{68}Ga-PSMA-11 PET biodistribution studies in tumour-bearing mice demonstrated a rapid tracer clearance from circulation and indicated a high ^{68}Ga-PSMA-11 uptake in PSMA-expressing tumour lesions within the first minutes after tracer injection [29]. To date, in only one study in one single patient earlier ^{68}Ga-PSMA-uptake in a PC lesion compared to accumulation in the urinary bladder was described on dynamic PET imaging performed in the first 60 min p.i. [30].

The primary objective of our study was to assess tumour targeting and pharmacokinetic properties of ^{68}Ga-PSMA-11 within 0–8 min after injection in a larger number of PC patients. We investigated if time-activity curves (TAC) derived from early tracer kinetics allow differentiating pathologic lesions suggestive of PC from physiologic urinary bladder activity. The second goal was to evaluate whether early dynamic PET-acquisition (edPET) could increase diagnostic performance of ^{68}Ga-PSMA-11 PET in detecting LR in PC patients with BR.

Materials and methods

A total of 80 consecutive PC patients who were referred to our department for a ^{68}Ga-PSMA-11 PET/CT from November 2013 to December 2014 were retrospectively analysed. In 64 patients ^{68}Ga-PSMA-11 PET/CT was performed because of BR after primary therapy with RP or radiotherapy. Eight patients were referred for ^{68}Ga-PSMA-11 PET/CT for primary staging after diagnosis of PC was confirmed by transrectal ultrasound (TRUS) guided biopsy. Eight patients were sent for ^{68}Ga-PSMA-11 PET/CT for evaluation of therapy response and restaging in known PC. We decided not to limit the study to PC patients with BR but also to include patients with known PC lesions in order to enhance the power of the statistical analysis. Patient characteristics are shown in detail in Table 1. The study was conducted according to the principles of the Declaration of Helsinki and its subsequent amendments [31]. Written informed consent was obtained from all patients according to institutional guidelines.

Radiopharmaceutical

PSMA-11 (Glu-NH-CO-NH-Lys(Ahx)-HBED-CC; HBED = N,N'-bis[2-hydroxy-5-(carboxyethyl)benzyl]ethylenediamine-N, N′-diacetic acid) was obtained from ABX advanced biochemical compounds (Radeberg, Germany) in GMP quality. ^{68}Ga-PSMA-11 was prepared in a procedure similar to that described by Eder et al. [32], and transferred to a cassette-based automated synthesis module (Modular-Lab PharmTracer; Eckert & Ziegler, Berlin) based on "acetone-free" cation exchange postprocessing [33]. Briefly, ^{68}Ga-chloride was obtained by elution of a ^{68}Ge/^{68}Ga generator (IGG100; Eckert & Ziegler, Berlin; 1850 MBq reference activity) with 6 mL 0.1 N HCl and absorbed on a SCX cation exchange cartridge. The activity was eluted from the cartridge with a concentrated NaCl/HCl solution and added to 10 µg PSMA-11, 50 µL 0.2 M ascorbic acid and 0.4 mL 2 M sodium acetate buffer, pH 4.5, to a total volume of 1–1.5 mL. The resulting solution was heated to 95 °C for 10 min, diluted with saline and transferred to a C-18 reversed-phase cartridge. ^{68}Ga-PSMA was eluted with 1 mL ethanol/water (1:1) and diluted with 7 mL physiological saline solution through a low protein sterile filter. The resulting solution contained >400 MBq ^{68}Ga-PSMA (with an average radiochemical yield of >80%), and <10% ethanol in physiological saline solution. Quality control procedures were applied following the European Pharmacopoeia monograph "^{68}Ga-Edotreotide injection" including tests for identity, radiochemical purity, ^{68}Ge, and ethanol content,

Table 1 Patient characteristics

	Group 1 BR	Group 2 Primary staging	Group 2 Therapy response/Restaging
Patients (n)	64	8	8
Primary RP	56	–	4
Primary radiation therapy	8	–	–
Age median (range) in years	69 (57–92)	68 (47–77)	69 (60–72)
Primary Gleason score median (range)	7 (6–9)*	8 (7–10)	8 (6–9)
PSA (ng/ml) median (range)	1.7 (0.2–35.1)**	20.8 (13.0–86.0)	10.5 (2.0–244.2)
Salvage radiation therapy	29	–	2
ADT at PET-scan	14	–	4

*In three of 64 patients no PSA within 8 weeks before ^{68}Ga-PSMA-11 PET was available

**In 13 of 64 patients no initial Gleason score could be obtained

RP radical prostatectomy, *ADT* androgen deprivation therapy

sterility and endotoxins. Reversed-phase HPLC revealed two major diastereomeric peaks of ^{68}Ga-PSMA-11 with a radiochemical purity of >92% and <2% free ^{68}Ga^{3+}. The absence of colloidal ^{68}Ga was proved by TLC.

Imaging protocol

^{68}Ga-PSMA-11 PET/CT imaging was performed in a dual-phase mode using a dedicated PET/CT system (Discovery 690; GE Healthcare, Milwaukee, WI, USA). The acquisition protocol included an early dynamic imaging of the pelvis centered on the prostate bed (one bed position with an axial field-of-view of 15.6 cm) starting immediately after intravenous injection of ^{68}Ga-PSMA-11 (median activity: 150 MBq, range 90–202 MBq). Dynamic images were acquired for 8 min with 60 s per frame collected in list mode. For attenuation correction and anatomic localisation a low-dose CT of the same region was acquired before tracer injection. Sixty minutes after tracer injection, a whole-body PET scan (skull base to upper thighs) in three-dimensional mode was acquired (emission time 2 min per bed position with an axial field-of-view of 15.6 cm per bed position). In 45 patients a low-dose CT scan was performed for attenuation correction of the PET emission data. The low-dose CT scan parameters using "GE smart mA dose modulation" were: 100 kVp, 15–150 mA, noise index 60, 0.8 s per tube rotation, slice thickness 3.75 mm, and pitch 1.375. Reconstruction was performed with an ordered subset expectation maximization algorithm (OSEM) with four iterations/eight subsets. In 35 patients (43.8%) a diagnostic contrast-enhanced CT (ceCT) scan was performed. The ceCT scan parameters using "GE smart mA dose modulation" were: 100–120 kVp, 80–450 mA, noise Index 24, 0.8 s per tube rotation, slice thickness 3.75 mm, and pitch 0.984. A CT scan of the thorax, abdomen and pelvis (shallow breathing) was acquired 40–70 s after injection of contrast agent (60 to 120 mL of Iomeron 400 mg/L, depending on patient body

weight), followed by a CT scan of the thorax in deep inhalation.

Image analysis

All ^{68}Ga-PSMA PET/CT images were analysed with dedicated commercially available software (Hybrid Viewer, Hermes Medical Solutions, Stockholm), which allowed the review of PET, CT, and fused imaging data in axial, coronal, and sagittal slices. PET images were interpreted independently by two board approved nuclear medicine physicians with more than 10 years of clinical experience, who were aware of all clinical data available. Any disagreement was resolved by consensus. In a first step, whole-body images 60 min p.i. were analysed. Any focal uptake higher than surrounding background activity that did not correspond to physiologic tracer accumulation was considered pathologic and suggestive of malignancy. This interpretation criteria is the result of our clinical experience and goes in line with published literature [20–22]. A quantitative cut-off for PC lesions was not described so far. In addition, semiquantitative analysis of all lesions visually considered typical for malignancy was performed using the maximum standardized uptake value (SUV$_{max}$). SUV$_{max}$ was chosen because SUV$_{mean}$ depends on the volume of interest drawn by the investigator, whereas SUV$_{max}$ is operator independent [30]. For calculation of the SUV$_{max}$ volumes of interest (VOIs) were drawn automatically centered on pathological lesions with focally increased uptake and a manually adapted isocontour threshold. In edPET images were analysed, visually using the same software described above (Hybrid Viewer, Hermes Medical Solutions, Stockholm) that allowed evaluation of acquired images frame by frame (eight frames with 60 s) fused with low-dose CT. Each lesion with focally increased uptake not representing physiologic uptake was counted and analysed semiquantitatively with SUV measurements. Only pathologic lesions that were present on whole-body PET and within the field of view of edPET were taken

into account. SUV_{max} was calculated within VOIs that were placed over the sites of pathologic tracer accumulation consistent with tumour lesions (prostate bed, LN, bone). In addition, SUV_{max} of areas with physiologic tracer uptake was measured in the urinary bladder, inguinal vessels, gluteal muscle, normal bone, and normal tissue in prostate bed/vesicourethral anastomosis/seminal vesicles. The latter served as a negative control group and was chosen because most of LR occur at that site, only regions with no apparent pathology were included. TAC of edPET describing SUV_{max} values versus time of pathologic lesions and areas with physiologic tracer uptake were derived.

Statistical analysis

^{68}Ga-PSMA-tracer uptake in PCa lesions versus tracer accumulation in the urinary bladder was compared with Wilcoxon signed rank-sum test for paired observations at each time-point. To account for the multiple testing problem (eight different time-points; therefore, eight single tests), p-values were corrected according to the Bonferroni method. Analyses were repeated for different subgroups. For visualization of the differences, TAC were generated. PSA-values were compared between PET-positive and negative patients using Mann–Whitney U test. A significance level of $\alpha = 0.05$ (2-tailed) was applied. Statistical analyses were performed using SPSS, version 22.0 (IBM Corp., Armonk, NY, USA).

Results

In 80 patients a total of 78 lesions with pathologic ^{68}Ga-PSMA-ligand uptake in the pelvis could be detected on whole-body PET 60 min p.i. that were within the field of view of edPET (prostatic fossa/prostate gland: $n = 27$; lymph nodes: $n = 35$; bone lesions: $n = 16$).

For evaluation we divided the patients in two subgroups. Group 1 comprised PC-patients with BR ($n = 64$), while group 2 consisted of PC patients referred for primary staging and response evaluation/restaging ($n = 16$).

In group 1, 13 out of 64 patients (20%) showed a pathologic lesion in the prostate bed 60 min p.i. consistent with LR (median SUV_{max} 60 min p.i.: 13.7). All of these patients demonstrated also a pathologic tracer uptake at the same location on edPET. Tracer uptake started at a very early time point of the dynamic imaging series, judged positive in all the patients within the first 3 min (median SUV_{max} 3 min: 5.0) with intensity constantly increasing until the end of the dynamic study (median SUV_{max} 8 min: 8.7). In 22 patients of group 1 a total of 27 lymph nodes (LN) with pathological tracer uptake in the pelvic region on images 60 min p.i. were revealed that were also in the field of view of edPET. However, SUV measurements on dynamic images could be obtained in only eight LN out of eight patients. In the remaining lymph nodes LN-related

tracer uptake could not be clearly discriminated from adjacent blood pool activity of iliacal vessels in the first minutes of acquisition and, therefore, were not included for SUV measurements. LN considered for SUV measurements showed a pathologic tracer uptake within the first 3 min (median SUV_{max} 3 min: 6.7), rising constantly to a median SUV_{max} of 10.2 until the end of dynamic acquisition. Pathologic bone lesions regarded as metastases present in the field of view on edPET were not found in group 1.

Considering group 2 (non BR), 14 out of 16 patients (87.5%) demonstrated a pathologic tracer uptake in the prostate gland/prostate fossa 60 min p.i. with a median SUV_{max} of 15.4. All of them also revealed a pathologic tracer accumulation on edPET at the same area. A pathologic tracer uptake in all lesions was observed within the first 3 min (median SUV_{max} 3 min: 5.6) exhibiting a median SUV_{max} of 8.2 at 8 min. With respect to LN evaluation eight LN with pathologic ^{68}Ga-PSMA-11 uptake in the pelvic region on whole-body PET were found in six patients. In onlyfour of these LN SUV-calculation on edPET was possible, due to disturbing uptake in adjacent iliacal vessels mentioned above. Pathologic tracer accumulation in these four LN was seen within the first 3 min (median SUV_{max} 3 min: 7.8), showing a median SUV_{max} of 9.9 at min 8 (median SUV_{max} of LN on SI: 20.5). As for bone metastases, in four patients a total of 16 pathologic bone lesions in the pelvic region were found 60 min p.i. (median SUV_{max}: 21.8). All of them were also visualised on edPET within the first 3 min (median SUV_{max} 3 min: 10.5) with intensity increasing until the end of dynamic imaging (median SUV_{max} 8 min: 14.9).

Pathologic lesions consistent with LR in group 1 could be verified in 11 out of 13 patients, confirmed either histologically ($n = 3$) or with MRI/CT ($n = 4$) or with follow-up ^{68}Ga-PSMA-11 PET/CT ($n = 2$). two 2 patients salvage radiotherapy of the prostatic fossa was performed with decreasing PSA, thereafter indicating a true positive finding. In two patients verification was not possible because both patients received androgen deprivation therapy after ^{68}Ga-PSMA-11 PET/CT and follow-up imaging was not available. Two LN with pathological tracer uptake could be verified histologically, two LN were classified as pathologic on ceCT, and for the remaining four LN no verification was possible (partly due to the small size of LN judged insuspicious on conventional imaging).

In group 2 pathologic lesions in the prostate gland/ prostate bed ($n = 14$) were either verified histologically with TRUS-biopsy ($n = 8$), showed a pathologic correlate in CT/MRI ($n = 4$) or were confirmed with follow-up ^{68}Ga-PSMA-11 PET/CT ($n = 2$). Pathologic bone lesions ($n = 16$) could not be verified histologically, but were positive on ceCT ($n = 11$) and/or confirmed on follow-up ^{68}Ga-PSMA-ligand PSMA-PET/CT. PSMA-positive LN were confirmed with follow-up imaging.

In comparison, urinary bladder activity assessed in all 80 patients was not detectable within the first 3 min on edPET, starting to become faintly visible in some patients only 5 min p.i. (median SUV_{max} 5 min: 1.6) increasing until the end of the dynamic study (median SUV_{max} 8 min: 4.3). In the statistical analysis pathologic radiotracer uptake in all tumour lesions ($n = 55$) was significantly higher until 6 min p.i. compared to urinary bladder activity (see Table 2). Regarding only the pathologic lesions in the prostate bed/gland ($n = 27$) revealed the same result (see Table 3) and the same was true considering all pathologic bone lesions and all pathologic LN separately (see supplement). TAC of pathologic lesions and urinary bladder activity are demonstrated in Fig. 1a. Inquinal vessel uptake showed a decreasing uptake pattern on edPET with the highest SUV_{max} within 1 min p.i. (median SUV_{max} 1 min: 8.1; median SUV_{max} 8 min: 2.7). Background activity of gluteal muscle increased within the first minutes and reached a plateau thereafter; however, never exceeding a median SUV_{max} of 1.6. SUV-measurements of the vesicourethral anastomosis/seminal vesicle region revealed a TAC similar to gluteal muscle activity with a median SUV_{max} not higher than 2.2 at all time frames of edPET. Respective SUV_{max} values of the regions with physiologic tracer uptake are listed in Table 4. TAC comparing tumour lesions to normal tissue are shown in Fig. 1b.

In summary, all pathologic PSMA-positive lesions that could be included in semiquantitative analysis showed a typical accumulation type TAC with an early onset of radiotracer uptake on edPET that differed clearly from the uptake pattern in the urinary bladder, as well as in normal tissue (see patient on Fig. 2).

Using these characteristic shapes of TAC with an early PSMA-11 uptake and a rising TAC-pattern on edPET as criteria typical for malignancy in a second step we reevaluated the prostatic fossa of all 64 PC-patients referred for BR (group 1). In six patients (9.4%) who were judged negative or equivocal for LR on whole-body PET 60 min p.i., pathologic tracer accumulation in the prostate bed adjacent to the urinary bladder was detected on edPET, representing a finding highly suspicious of LR. An example of a patient with an equivocal finding 60 min p.i. and a clear positive lesion in the prostate bed on edPET is shown in Fig. 3. In four of these patients LR was confirmed with ceCT/MRI ($n = 2$), with follow-up imaging ($n = 1$) and a falling PSA after salvage radiotherapy to the prostate bed ($n = 1$). In 2 patients no validation of the findings of edPET could be obtained. In 9 patients (14.1%) with an equivocal finding in the prostatic fossa 60 min p.i. no pathologic tracer uptake on edPET was found, making a LR unlikely. In four of these nine patients, follow-up imaging could not demonstrate LR, one patient received RT of the prostate bed with no adequate fall of PSA thereafter, and in the remaining four patients no follow-up data were available to confirm the negative finding on edPET. In total in 23.5% of PC patients with BR the findings obtained by edPET helped to distinguish tracer activity in the urinary bladder and urethra from probable pathologic tracer-uptake in the prostatic fossa.

Correlation of PSA-values and PET-positivity regarding LR demonstrated that the median PSA-value of patients judged negative for LR was significantly lower than in patients in whom LR could be detected (1.0 vs. 4.8 ng/mL; $p = 0.01$). The median PSA value of the subgroup positive only on edPET was lower than in patients who revealed a positive finding on both edPET and on whole-body PET

Table 2 SUV_{max} values of all ^{68}Ga-PSMA-11 positive tumour lesions and urinary bladder

	Total tumour lesions, group 1 + 2 ($n = 55$)					Urinary bladder activity				p-value*
	Median SUV_{max}	95% CI for median	Mean	SD	Range	Median SUV_{max}	Mean	SD	Range	
1 min	2.9	2.5–3.3	4.0	3.5	0.3–14.8	0.5	0.6	0.3	0.0–1.2	<0.001
2 min	5.5	4.5–7.5	7.1	4.5	1.9–24.1	1.1	1.2	0.6	0.4–2.8	<0.001
3 min	6.3	5.6–8.5	9.0	6.0	2.3–27.2	1.3	1.3	0.5	0.5–2.2	<0.001
4 min	7.5	6.4–8.9	10.4	7.0	3.1–29.2	1.2	1.4	0.7	0.5–3.3	<0.001
5 min	7.7	6.9–10.1	10.9	7.3	2.3–31.0	1.6	1.7	0.7	0.9–3.2	<0.001
6 min	8.5	7.1–10.7	11.7	7.8	3.1–33.1	2.0	2.9	2.3	0.8–10.6	<0.001
7 min	9.1	8.0–10.9	12.4	8.1	3.1–36.0	3.0	5.5	7.5	1.3–33.2	1.000
8 min	10.3	9.2–11.9	13.2	8.6	4.5–44.4	4.3	8.4	12.3	1.6–57.0	1.000
60 min	15.7	–	21.3	17.6	4.6–115.5	–	–	–	–	–

1 min to 8 min representing each time frame of early dynamic PET. 60 min: SUV_{max} value of tumour lesions on whole-body PET 60 min p.i.. (Tables of urinary bladder activity compared to lesions in prostate bed/gland, lymph nodes and bone of group 1 and 2 separately are listed in supplement 1–6)

*: p-value from Wilcoxon rank-sum test for paired observations; corrected for multiple testing according to the Bonferroni method

SD standard deviation, *CI* confidential interval

Table 3 SUV_{max} values of all ^{68}Ga-PSMA-11 positive tumour lesions in the prostate bed/prostate gland and urinary bladder

	Tumour lesion prostate, group 1 + 2 ($n = 27$)					Urinary bladder activity				p-value*
	Median SUV_{max}	95% CI for median	Mean	SD	Range	Median SUV_{max}	Mean	SD	Range	
1 min	2.0	1.6–2.8	2.5	1.7	0.3–9.5	0.5	0.6	0.3	0.0–1.2	<0.001
2 min	4.7	4.3–5.1	5.4	2.5	1.9–12.7	1.1	1.1	0.5	0.4–2.8	<0.001
3 min	5.5	5.0–5.9	6.6	3.4	2.3–16.0	1.2	1.2	0.5	0.5–2.2	<0.001
4 min	6.4	5.2–6.8	7.7	4.7	4.1–23.7	1.2	1.3	0.7	0.5–3.3	<0.001
5 min	6.2	5.9–7.5	8.1	4.5	2.9–20.4	1.5	1.7	0.7	0.9–3.2	<0.001
6 min	6.8	6.1–7.9	8.7	4.8	3.8–23.7	2.0	2.6	2.0	1.0–10.6	<0.001
7 min	7.5	6.2–9.0	9.2	5.1	4.4–24.5	3.0	3.9	3.9	1.3–20.9	<0.001
8 min	8.7	6.7–9.9	10.0	5.3	4.5–24.5	4.3	6.0	5.5	1.6–27.9	0.017
60 min	15.1	–	19.0	14.6	5.2–66.4	–	–	–	–	–

1 min to 8 min representing each time frame of early dynamic PET. 60 min: SUV_{max} value of tumour lesions on whole-body PET 60 min p.i

*: p-value from Wilcoxon rank-sum test for paired observations; corrected for multiple testing according to the Bonferroni method

SD standard deviation, *CI* confidential interval

60 min p.i. (3.5 vs. 4.8 ng/mL); however, a statistical significant difference could not be shown ($p = 0.210$).

Discussion

We conducted a retrospective study in order to investigate the feasibility and potential benefit of early dynamic acquisition in PC patients referred for ^{68}Ga-PSMA-11 PET/CT.

Although until now in ^{68}Ga-PSMA-11 PET no standard imaging protocol was defined, whole-body PET acquistion 60 min p.i. is usually applied in clinical routine [26]. However, at this time point intense physiological urinary bladder accumulation is present [26, 28]. Small local recurrences adjacent to the bladder might be overlooked. In order to improve the assessment of areas in the vicinity of the urinary

bladder, several ways to reduce urinary bladder activity are described. Methods such as administration of diuretics, voiding the bladder directly before the PET exam, or starting PET acquisition from the thigh do not reduce urinary bladder activity sufficiently [30]

Therefore, the primary aim of the study was to analyse ^{68}Ga-PSMA-11 pharmacokinetics on early dynamic PET-acquisition and to explore whether by means of time–activity curves it is possible to differentiate PC lesions from urinary bladder activity. In a recently published study Sachpekidis et al. performed dynamic ^{68}Ga-PSMA-11 PET imaging during the first 60 min of PET acquisition in 24 PC patients referred for primary staging. They could demonstrate that ^{68}Ga-PSMA-11 uptake in PC lesions constantly increased on dynamic PET-imaging. PC related ^{68}Ga-PSMA-11 uptake was significantly higher than tracer accumulation in normal

Fig. 1 Time-activity curves of pathologic lesions compared to urinary bladder activity (*1a*) and time-activity curves of pathologic lesions compared to physiologic radiotracer uptake in normal tissue (*1b*)
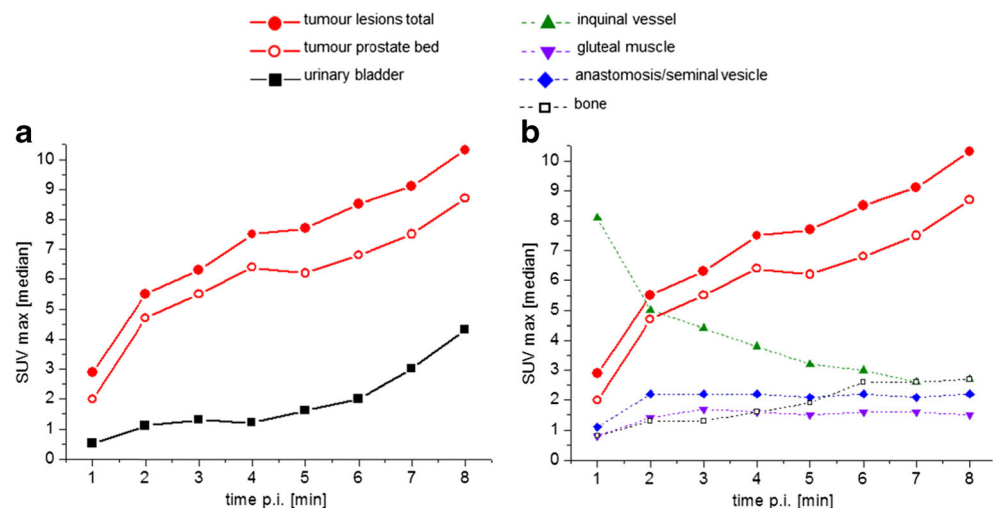
Table 4 SUV$_{max}$ values of tissues with physiologic ^{68}Ga-PSMA-11 tracer uptake

	Inquinal vessel		Gluteal muscle		Anastomosis/seminal vesicle		Normal bone	
	Median SUV$_{max}$	Range	Median SUV$_{max}$	Range	Median SUV$_{max}$	Range	Median SUV$_{max}$	Range
1 min	8.1	2–13.1	0.8	0.1–1.7	1.1	0.1–1.9	0.8	0.8–1.6
2 min	5.0	3.0–8.0	1.4	0.6–3.9	2.2	0.9–4.1	1.3	1.4–2.0
3 min	4.4	2.3–7.3	1.7	0.6–3.5	2.2	1.2–3.8	1.3	1.7–2.4
4 min	3.8	2.3–6.5	1.6	0.5–3.1	2.2	1.1–3.3	1.6	1.6–2.5
5 min	3.2	1.9–5.6	1.5	0.4–2.7	2.1	1.3–3.5	1.9	1.5–2.2
6 min	3.0	1.4–5.4	1.6	0.4–2.8	2.2	1.1–3.5	2.6	1.4–1.7
7 min	2.6	1.6–4.7	1.6	0.4–2.5	2.1	1.3–3.8	2.6	1.3–1.7
8 min	2.7	1.7–4.7	1.5	0.4–2.5	2.2	1.0–3.4	2.7	1.3–1.8

1 min to 8 min representing each time frame of early dynamic PET

prostate tissue. However, they did not investigate ^{68}Ga-PSMA-11 pharmacokinetics of the urinary bladder [34]. To the best of our knowledge this is the first study to assess ^{68}Ga-PSMA-11 pharmacokinetics of pathologic and physiologic uptake on early dynamic imaging within the first 8 min p.i. comparing PC-related uptake to urinary bladder activity in a larger cohort of PC patients. To date, for only one single patient earlier ^{68}Ga-PSMA-11 uptake in a PC recurrence lesion
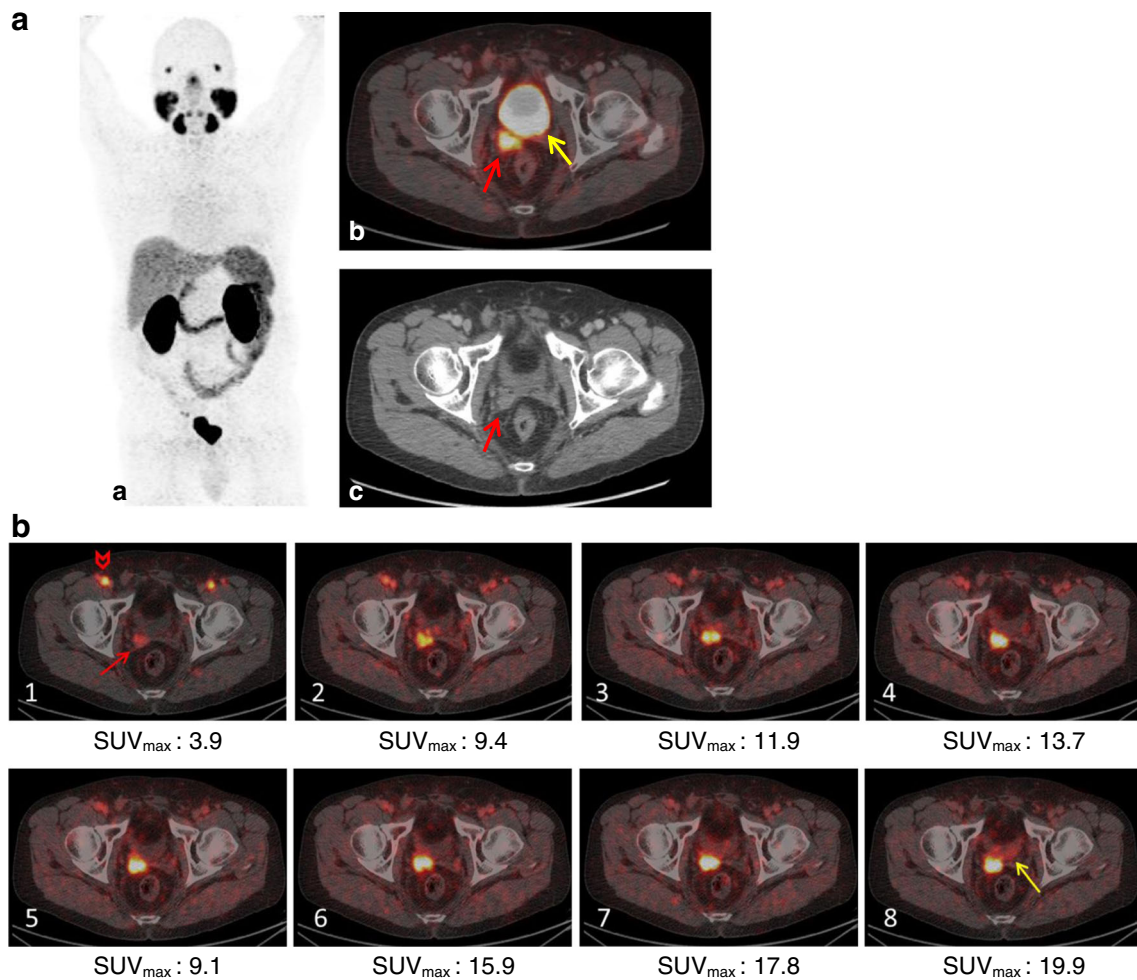

Fig. 2 **a** ^{68}Ga-PSMA-11 PET/CT in a PC patient with biochemical recurrence (PSA: 2.2 ng/mL). **b** Maximum intensity projection (**a**), fused PET/CT (**b**), and ceCT (**c**) of whole-body PET 60 min p.i. with a pathologic lesion in the right seminal vesicle on fused PET/CT (SUVmax: 48.2) and corresponding nodular lesion with faint contrast enhancement on CT (*red arrows*), *yellow arrow*: urinary bladder activity
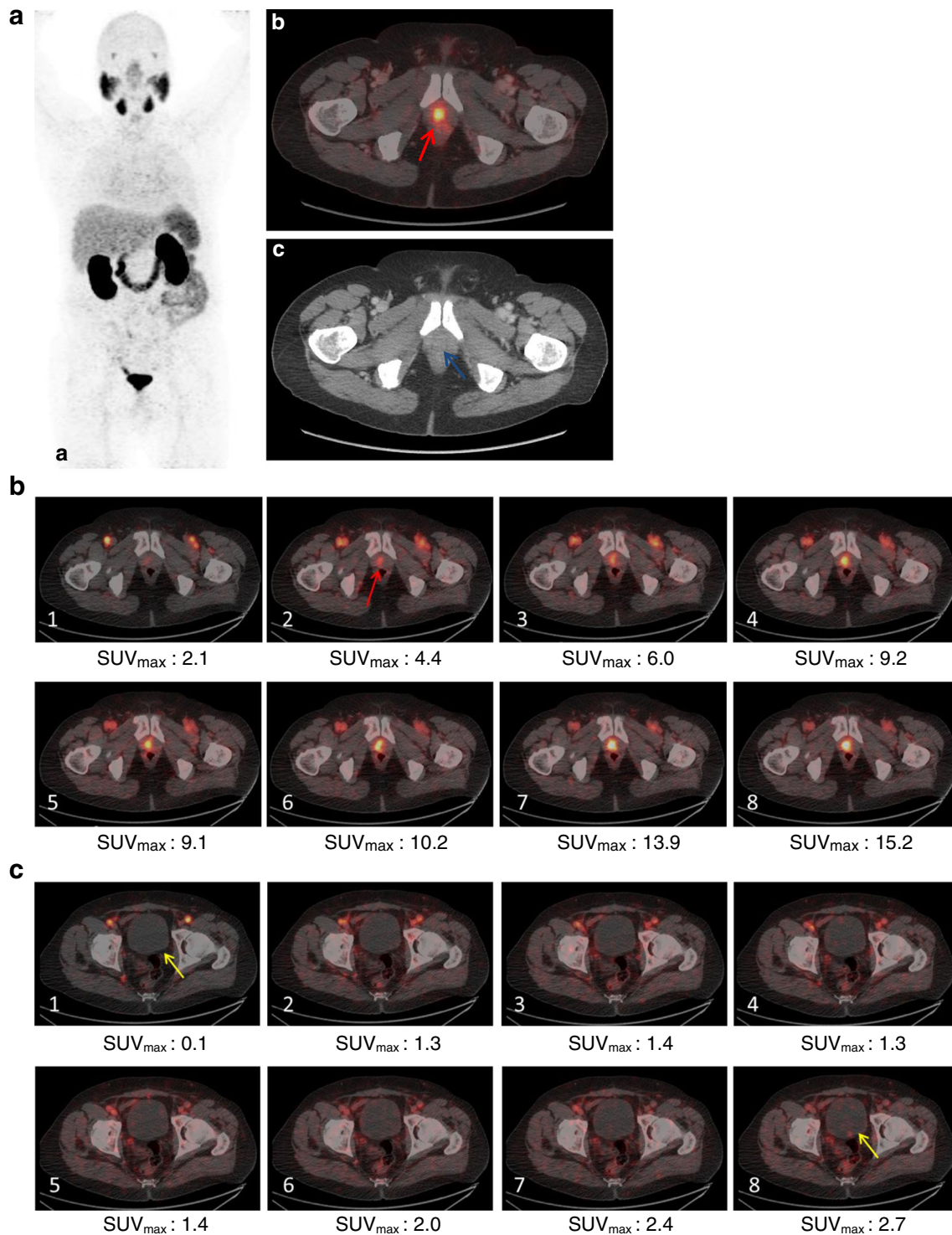
Fig. 3 **a** ^{68}Ga-PSMA-11 PET/CT of a PC patient with biochemical recurrence (PSA: 4.46 ng/mL). **b** Maximum intensity projection (**a**), fused PET/CT (**b**), and ceCT (**c**) with markedly increased tracer accumulation adjacent to the urinary bladder (*red arrow*) with no pathologic finding on CT (*blue arrow*). A differentiation of physiologic urethra activity and local relapse was not possible. **c** Early dynamic PET comprising pelvic region of patient on Fig. 3a with fused PET/CT (low-dose CT) displaying an early and constantly rising focal tracer uptake at the same area (*red arrow*), a finding highly suspicious for local recurrence. Images 1–8 representing min 1–8 post injection and corresponding SUV$_{max}$ value listed below image. **d** Early dynamic PET comprising pelvic region of patient on Fig. 3a with fused PET/CT (low-dose CT) displaying a slice centered on urinary bladder (*yellow arrow*): absent radiotracer activity in the urinary bladder in first 5 min and starting to become faintly visible 6 min p.i

compared to accumulation in the urinary bladder on dynamic PET-imaging was described [30].

Kabasakal et al. performed early static imaging of the pelvis 5 min p.i. in a series of 28 PC patients referred to PSMA-PET for assessment of BR or staging of primary tumour describing significant tracer uptake in PC lesions at that time point [35]. Although tumour related tracer uptake was significantly lower on early images compared to whole body imaging 60 min p.i. assessment of the prostate bed was found easier on early images, due to absent bladder activity.

This observation goes in line with the findings of our study. All pathologic lesions suggestive of PC that were evaluated ($n = 55$) demonstrated an increased tracer accumulation within the first 3 min of edPET when tracer activity within the urinary bladder was still not visible in all of the patients. Tracer accumulation in the urinary bladder started to become discernable only 5 min p.i. in some patients. Median SUV_{max} of all tumour lesions ($n = 55$) in the time frames 1–6 min p.i. was significantly higher than in the urinary bladder ($p < 0.001$). This was also the case when only pathological lesions in the prostate bed/prostate gland ($n = 27$) were considered. TAC of lesions consistent with PC showed a characteristic course with a steep early onset of tracer accumulation within 1–2 min p.i. and a constant ascent until the end of edPET. TAC of the urinary bladder in contrast showed a late onset of radiotracer accumulation starting to rise at min 5. We also evaluated radiotracer uptake on edPET in normal tissue to exclude unspecific effects of tracer uptake found in PC lesions. Blood pool activity measured over inquinal vessels showed a high radiotracer uptake within the first minutes with the highest median SUV_{max} at min 1. However, compared to pathologic PC lesions TAC of vessel activity showed a steep descent until 8 min p.i.. TACS of background activity measured over gluteal muscle, in the vesicourethral anastomosis/seminal vesicle where no pathology was present and over normal bone exhibited a low ascent in the first minutes, reaching a plateau thereafter. We could demonstrate that the urinary bladder and normal tissue showed a different behavior of ^{68}Ga-PSMA-ligand uptake in the first 8 min p.i. compared to pathologic prostate lesions. On edPET evaluation of the prostate bed was not hampered by adjacent bladder activity, as is the case on whole body imaging 60 min p.i.

The second goal of the study was to evaluate whether integration of edPET and the application of the different TAC pattern mentioned above could enhance diagnostic performance of ^{68}Ga-PSMA-11 PET/CT. In PC patients with BR detection of local relapse at an early stage is a prerequisite for a successful SRT [3]. ^{68}Ga-PSMA-11 PET/CT has shown high overall accuracy in detecting recurrent PC [20–22]. However, detection rates of LR of up to 35.1% of patients using a standard acquistion protocol with imaging 60 mi p.i.

seem relatively low [20, 21]. With ^{18}F-choline PET early dynamic acquisition of the pelvic region within the first 8 min p.i. helps to distinguish LR from urinary bladder activity and is generally accepted part of the standard ^{18}F-choline PET acquisition protocol in the assessment of PC-patients with BR [36, 37]. Simone et al. demonstrated a significant increase in diagnostic accuracy in ^{18}F-choline PET with the help of early dynamic phase compared to standard whole body imaging 10–20 min post injection. The majority of LR were only visible on early dynamic images, resulting in a detection rate of LR in 67.1% of patients [9].

With respect to the detection rate of PC in the prostatic fossa, Kabasakal et al. could not find a difference between early static images 5 min p.i. and late imaging 60 min p.i. in ^{68}Ga-PSMA-ligand PET [35]. The lack of difference in the detection rate between the two phases found by this group may be partially contributed to the fact that only eight patients with BR after operation and/or radiotherapy were included in the study, with relatively high PSA values (median PSA: 10.59 ng/mL) representing high tumour volume that in our experience is easier to discriminate on whole-body PET 60 min p.i.. Nonetheless, Kabasakal et al. concluded that early images could be helpful in the assessment of the prostate bed and structures in the proximity of the urinary bladder.

In our study in the subgroup of patients evaluated for BR ($n = 64$) in 9.4% of cases an early focal tracer uptake in the prostate bed suggestive of LR could be found that was concealed by high radioactivity in the urinary bladder 60 min p.i.. Furthermore, with regard to assessment of LR, in our experience equivocal findings in areas close to urinary bladder are quite common on whole-body PET 60 min p.i.. In fact, in 14.1% of our patient cohort with BR LR adjacent to the urinary bladder could not be ruled out on images 60 min p.i.. However, as there was no pathologic tracer uptake within the first minutes of ed PET suggestive of malignancy, we concluded that LR was unlikely. Thus, in 23.5% of patients edPET contributed to the final interpretation of ^{68}Ga-PSMA-ligand PET. The detection rate of LR with whole-body PET 60 min p.i. alone and in combination with edPET was 20.3 and 29.7%, respectively. The still somewhat low detection rate in comparison to other studies and MRI may be partially contributed to the fact that patients evaluated for BR in our study had a relatively low PSA value (median PSA: 1.7 ng/mL) including 24 patients with PSA <1.0 ng/mL. In addition we also assessed whether median PSA values of patients positive for LR only on edPET differed from those who were positive on both edPET and whole-body PET 60 min p.i.. The median PSA-value of patients who showed LR only on edPET was lower (3.5 vs. 4.8 ng/mL); however, it did not reach statistical significance ($p = 0.210$).

As verification of positive findings on edPET not visible on whole-body PET 60 min p.i. was not available in all the cases the results have to be interpreted with caution. Further analyses with larger patient cohorts are required to correlate lesions that are judged pathologic only on edPET with other imaging modalities (MRI, TRUS) and preferably with histology, in order to address the question if they represent true positive PC lesions.

Despite this major limitation, the results of our study are encouraging enough to recommend application of edPET in addition to whole body PET 60 min p.i. in all PC patients with BR referred for ^{68}Ga-PSMA-11 PET/CT. Our data indicate that early dynamic imaging might increase the detection rate of LR compared to image acquisition 60 min p.i. alone.

Conclusions

With this study we could demonstrate that early dynamic imaging in ^{68}Ga-PSMA-11 PET/CT in PC-patients can reliably discriminate pathologic tracer uptake in PC lesions from physiologic tracer accumulation in the urinary bladder. Early dynamic imaging improves the detection rate of LR in ^{68}Ga-PSMA-11 PET/CT. We conclude that early dynamic acquisition in combination with whole body imaging 60 min p.i. should be applied in PC patients with biochemical relapse referred for ^{68}Ga-PSMA-11 PET/CT.

References

1. Mottet N, Bellmunt J, Bolla M, Briers E, Cumberbatch MG, De Santis M, et al. EAU-ESTRO-SIOG Guidelines on Prostate Cancer. Part 1: screening, diagnosis, and local treatment with curative intent. Eur Urol. 2016. doi: 10.1016/j.eururo.2016.08.003.

2. Mullins JK, Feng Z, Trock BJ, Epstein JI, Walsh PC, Loeb S. The impact of anatomical radical retropubic prostatectomy on cancer control: the 30-year anniversary. J Urol. 2012;188(6):2219–24.

3. Cornford P, Bellmunt J, Bolla M, Briers E, De Santis M, Gross T, et al. EAU-ESTRO-SIOG Guidelines on Prostate Cancer. Part II: treatment of relapsing, metastatic, and castration-resistant prostate cancer. Eur Urol. 2016. doi: 10.1016/j.eururo.2016.08.002.

4. Scattoni V, Montorsi F, Picchio M, Roscigno M, Salonia A, Rigatti P, et al. Diagnosis of local recurrence after radical prostatectomy. BJU Int. 2004;93(5):680–8.

5. Scattoni V, Roscigno M, Raber M, Montorsi F, Da Pozzo L, Guazzoni G, et al. Multiple vesico-urethral biopsies following radical prostatectomy: the predictive roles of TRUS, DRE, PSA and the pathological stage. Eur Urol. 2003;44(4):407–14.

6. Cirillo S, Petracchini M, Scotti L, Gallo T, Macera A, Bona MC, et al. Endorectal magnetic resonance imaging at 1.5 Tesla to assess local recurrence following radical prostatectomy using T2-weighted and contrast-enhanced imaging. Eur Radiol. 2009;19(3): 761–9. doi:10.1007/s00330-008-1174-8.

7. De Visschere PJ, De Meerleer GO, Fütterer JJ, Villeirs GM. Role of MRI in follow-up after focal therapy for prostate carcinoma. AJR Am J Roentgenol. 2010;194(6):1427–33. doi:10.2214/AJR.10.4263. Review.

8. Picchio M, Briganti A, Fanti S, Heidenreich A, Krause BJ, Messa C, et al. The role of choline positron emission tomography/computed tomography in the management of patients with prostate-specific antigen progression after radical treatment of prostate cancer. Eur Urol. 2011;59(1):51–60. doi:10.1016/j.eururo.2010.09.004.

9. Simone G, Di Pierro GB, Papalia R, Sciuto R, Rea S, Ferriero M, et al. Significant increase in detection of prostate cancer recurrence following radical prostatectomy with an early imaging acquisition protocol with ^{18}F-fluorocholine positron emission tomography/computed tomography. World J Urol. 2015;33(10):1511–8. doi:10.1007/s00345-015-1481-z.

10. Evangelista L, Cimitan M, Hodolič M, Baseric T, Fettich J, Borsatti E. The ability of 18F-choline PET/CT to identify local recurrence of prostate cancer. Abdom Imaging. 2015;40(8):3230–7. doi:10.1007/s00261-015-0547-0.

11. Fanti S, Minozzi S, Castellucci P, Balduzzi S, Herrmann K, Krause BJ, et al. PET/CT with (11)C-choline for evaluation of prostate cancer patients with biochemical recurrence: meta-analysis and critical review of available data. Eur J Nucl Med Mol Imaging. 2016;43(1):55–69. doi:10.1007/s00259-015-3202-7.

12. Panebianco V, Sciarra A, Lisi D, Galati F, Buonocore V, Catalano C, et al. Prostate cancer: 1HMRS-DCEMR at 3T versus [(18)F]choline PET/CT in the detection of local prostate cancer recurrence in men with biochemical progression after radical retropubic prostatectomy (RRP). Eur J Radiol. 2012;81(4):700–8. doi:10.1016/j.ejrad.2011.01.095.

13. Alfarone A, Panebianco V, Schillaci O, Salciccia S, Cattarino S, Mariotti G, et al. Comparative analysis of multiparametric magnetic resonance and PET-CT in the management of local recurrence after radical prostatectomy for prostate cancer. Crit Rev Oncol Hematol. 2012;84(1):109–21. doi:10.1016/j.critrevonc.2012.01.006.

14. Kitajima K, Murphy RC, Nathan MA, Froemming AT, Hagen CE, Takahashi N, et al. Detection of recurrent prostate cancer after radical prostatectomy: comparison of 11C-choline PET/CT with pelvic multiparametric MR imaging with endorectal coil. J Nucl Med. 2014;55(2):223–32. doi:10.2967/jnumed.113.123018.

15. Ceci F, Herrmann K, Castellucci P, Graziani T, Bluemel C, Schiavina R, et al. Impact of 11C-choline PET/CT on clinical decision making in recurrent prostate cancer: results from a retrospective two-centre trial. Eur J Nucl Med Mol Imaging. 2014;41(12): 2222–31. doi:10.1007/s00259-014-2872-x.

16. Ghosh A, Heston WD. Tumor target prostate specific membrane antigen (PSMA) and its regulation in prostate cancer. J Cell Biochem. 2004;91(3):528–39.

17. Zaheer A, Cho SY, Pomper MG. New agents and techniques for imaging prostate cancer. J Nucl Med. 2009;50(9):1387–90.

18. Banerjee SR, Pullambhatla M, Byun Y, Nimmagadda S, Green G, Fox JJ, et al. 68Ga-labeled inhibitors of prostate-specific membrane antigen (PSMA) for imaging prostate cancer. J Med Chem. 2010;53(14):5333–41.

19. Lindenberg L, Choyke P, Dahut W. Prostate cancer imaging with novel PET tracers. Curr Urol Rep. 2016;17(3):18. doi:10.1007/s11934-016-0575-5.

20. Eiber M, Maurer T, Souvatzoglou M, Beer AJ, Ruffani A, Haller B, et al. Evaluation of hybrid ^{68}Ga-PSMA ligand PET/CT in 248 patients with biochemical recurrence after radical prostatectomy. J Nucl Med. 2015;56(5):668–74. doi:10.2967/jnumed.115.154153.

21. Ceci F, Uprimny C, Nilica B, Geraldo L, Kendler D, Kroiss A, et al. (68)Ga-PSMA PET/CT for restaging recurrent prostate cancer: which factors are associated with PET/CT detection rate? Eur J Nucl Med Mol Imaging. 2015;42(8):1284–94. doi:10.1007/s00259-015-3078-6.

22. Afshar-Oromieh A, Avtzi E, Giesel FL, Holland-Letz T, Linhart HG, Eder M, et al. The diagnostic value of PET/CT imaging with the (68)Ga-labelled PSMA ligand HBED-CC in the diagnosis of recurrent prostate cancer. Eur J Nucl Med Mol Imaging. 2015;42(2):197–209. doi:10.1007/s00259-014-2949-6.

23. Afshar-Oromieh A, Haberkorn U, Eder M, Eisenhut M, Zechmann CM. [68Ga]Gallium-labelled PSMA ligand as superior PET tracer for the diagnosis of prostate cancer: comparison with 18F-FECH. Eur J Nucl Med Mol Imaging. 2012;39(6):1085–6. doi:10.1007/s00259-012-2069-0.

24. Afshar-Oromieh A, Zechmann CM, Malcher A, Eder M, Eisenhut M, Linhart HG, et al. Comparison of PET imaging with a (68)Ga-labelled PSMA ligand and (18)F-choline-based PET/CT for the diagnosis of recurrent prostate cancer. Eur J Nucl Med Mol Imaging. 2014;41(1):11–20. doi:10.1007/s00259-013-2525-5.

25. Morigi JJ, Stricker PD, van Leeuwen PJ, Tang R, Ho B, Nguyen Q, et al. Prospective comparison of 18F-Fluoromethylcholine versus 68Ga-PSMA PET/CT in prostate cancer patients who have rising PSA after curative treatment and are being considered for targeted therapy. J Nucl Med. 2015;56(8):1185–90. doi:10.2967/jnumed.115.160382.

26. Afshar-Oromieh A, Hetzheim H, Kübler W, Kratochwil C, Giesel FL, Hope TA, et al. Radiation dosimetry of (68)Ga-PSMA-11 (HBED-CC) and preliminary evaluation of optimal imaging timing. Eur J Nucl Med Mol Imaging. 2016;43(9):1611–20. doi:10.1007/s00259-016-3419-0.

27. Demirci E, Sahin OE, Ocak M, Akovali B, Nematyazar J, Kabasakal L. Normal distribution pattern and physiological variants of 68Ga-PSMA-11 PET/CT imaging. Nucl Med Commun. 2016;37(11):1169–79. doi:10.1097/MNM.0000000000000566.

28. Rauscher I, Maurer T, Fendler WP, Sommer WH, Schwaiger M, Eiber M. (68)Ga-PSMA ligand PET/CT in patients with prostate cancer: how we review and report. Cancer Imaging. 2016;16(1):14. doi:10.1186/s40644-016-0072-6. Review.

29. Schäfer M, Bauder-Wüst U, Leotta K, Zoller F, Mier W, Haberkorn U, et al. A dimerized urea-based inhibitor of the prostate-specific membrane antigen for 68Ga-PET imaging of prostate cancer. EJNMMI Res. 2012;2(1):23. doi:10.1186/2191-219X-2-23.

30. Afshar-Oromieh A, Malcher A, Eder M, Eisenhut M, Linhart HG, Hadaschik BA, et al. PET imaging with a [68Ga]gallium-labelled PSMA ligand for the diagnosis of prostate cancer: biodistribution in humans and first evaluation of tumour lesions. Eur J Nucl Med Mol Imaging. 2013;40(4):486–95. doi:10.1007/s00259-012-2298-2.

31. World Medical Association Declaration of Helsinki: ethical principles for medical research involving human subjects. JAMA. 2000;284:3043–5.

32. Eder M, Neels O, Müller M, Bauder-Wüst U, Remde Y, Schäfer M, et al. Novel preclinical and radiopharmaceutical aspects of [68Ga]Ga-PSMA-HBED-CC: a new PET tracer for imaging of prostate cancer. Pharmaceuticals (Basel). 2014;7(7):779–96.

33. Mueller D, Klette I, Baum RP, Gottschaldt M, Schultz MK, Breeman WA. Simplified NaCl based (68)Ga concentration and labeling procedure for rapid synthesis of (68)Ga radiopharmaceuticals in high radiochemical purity. Bioconjug Chem. 2012;23(8):1712–7. doi:10.1021/bc300103t.

34. Sachpekidis C, Kopka K, Eder M, Hadaschik BA, Freitag MT, Pan L, et al. 68Ga-PSMA-11 Dynamic PET/CT imaging in primary prostate cancer. Clin Nucl Med. 2016;41(11):e473–9.

35. Kabasakal L, Demirci E, Ocak M, Akyel R, Nematyazar J, Aygun A, et al. Evaluation of PSMA PET/CT imaging using a 68Ga-HBED-CC ligand in patients with prostate cancer and the value of early pelvic imaging. Nucl Med Commun. 2015;36(6):582–7. doi:10.1097/MNM.0000000000000290.

36. Beheshti M, Langsteger W. PET imaging of prostate cancer using radiolabeled choline PET Clin. 2009;4(2):173–84. doi:10.1016/j.cpet.2009.06.003.

37. Steiner C, Vees H, Zaidi H, Wissmeyer M, Berrebi O, Kossovsky MP, et al. Three-phase 18F-fluorocholine PET/CT in the evaluation of prostate cancer recurrence. Nuklearmedizin. 2009;48(1):1–9. quiz N2-3.